

## A novel damage-tolerant superhydrophobic and superoleophilic material†

Xia Zhang,<sup>\*a</sup> Yonggang Guo,<sup>b</sup> Hengzhen Chen,<sup>a</sup> Wenzhong Zhu<sup>a</sup> and Pingyu Zhang<sup>a</sup>Cite this: *J. Mater. Chem. A*, 2014, 2, 9002Received 19th February 2014  
Accepted 18th March 2014

DOI: 10.1039/c4ta00869c

www.rsc.org/MaterialsA

A damage-tolerant superhydrophobic and superoleophilic bulk material is fabricated by a facile method. The novel bulk material demonstrates excellent resistance for oil fouling and can be used for water–oil separation. Different wettabilities have been realized on the material surface under UV irradiation, and the superhydrophobicity can be easily regenerated.

Superhydrophobic surfaces, which possess the virtue of having a large water contact angle (CA) and exhibit little sticking to water droplets, have numerous applications in self-cleaning,<sup>1,2</sup> non-wetting fabrics,<sup>3–5</sup> anti-fogging,<sup>6</sup> anti-icing,<sup>7,8</sup> buoyancy,<sup>9,10</sup> and water–oil separation.<sup>11–13</sup> However, the susceptibility to mechanical abrasion and oil fouling severely hinders the use of superhydrophobic surfaces in practical applications.<sup>14</sup> Mechanical abrasion on superhydrophobic surfaces will destroy the microscopic roughness features that are essential for superhydrophobicity. Furthermore, mechanical abrasion also removes the hydrophobic surface layer, causing a decline in their non-wetting behavior. Similarly, any oil contaminants penetrating into the textured surfaces are hard to remove and thus negate the superhydrophobic behavior.<sup>15,16</sup> Fabrication of superoleophobic surfaces should be an appealing way to suppress oil contamination, but this has proved extremely challenging. The challenge results from the difficulty in producing superoleophobic surfaces, which require some special structures and costly fluorochemicals to provide the needed surface roughness and surface energy. In addition, the superoleophobic surfaces are also fragile to mechanical contact because of their fine surface structures, making the surfaces lose their superoleophobicity easily.<sup>14–16</sup> Thus, seeking a

suitable way to solve the mechanical damage and oil fouling problems has been an urgent demand.

Despite the importance of mechanical durability in applications, less attention has been paid to the key issue until recently except for a few reported works.<sup>17–22</sup> Su *et al.* realized superhydrophobicity on an elastic material (polyurethane) to improve the abrasion resistance of the surface.<sup>21</sup> Zhang *et al.* prepared a superhydrophobic metal/polymer composite surface possessing both mechanical durability and easy repairability.<sup>20</sup> Fabricating a superhydrophobic bulk material possessing low-surface-energy microstructures extending throughout its whole volume is a new concept in designing damage-tolerant superhydrophobicity.<sup>19</sup> This concept is illustrated in Fig. 1. The bulk material will sustain the rough surface textures after mechanical abrasion, ensuring continued superhydrophobicity. Based on the above concept, in this work, we aim to fabricate a durable and robust superhydrophobic surface by a facile approach.

Polypropylene (PP), as an essential engineering polymer material, is used in many industrial applications. A pure PP surface does not show superhydrophobicity in the absence of surface texture roughness. In this communication, we demonstrate inorganic/PP composite bulk materials that rely on a dispersion of inorganic particle fillers to improve the surface

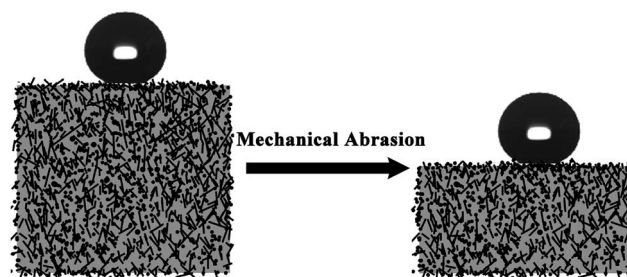


Fig. 1 Schematic illustration of a bulk material which can still sustain its superhydrophobicity after mechanical abrasion because of the low-surface-energy microstructures extending throughout its whole volume.

<sup>a</sup>Laboratory of Special Functional Materials, Henan University, Kaifeng 475001, China. E-mail: zx@henu.edu.cn

<sup>b</sup>School of Mechanical and Electrical Engineering, Henan University of Technology, Zhengzhou 450007, China

† Electronic supplementary information (ESI) available. See DOI: 10.1039/c4ta00869c

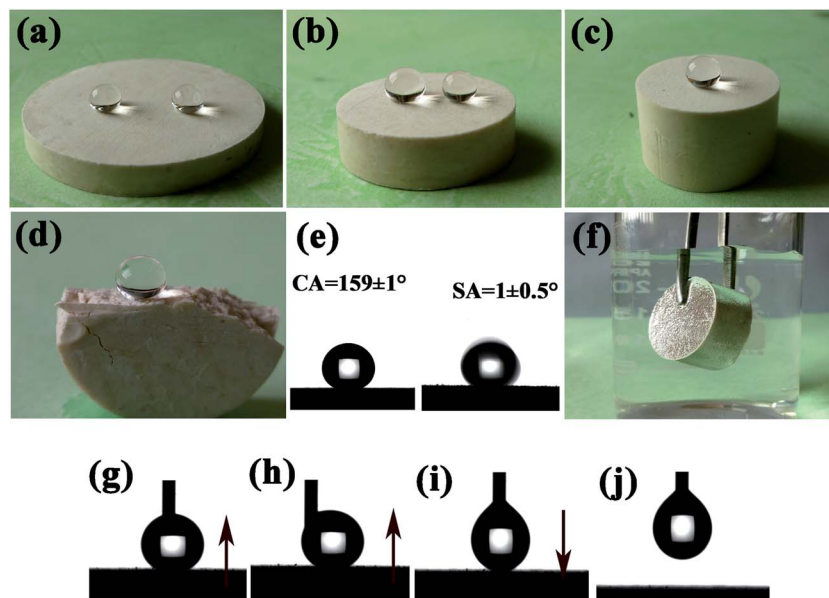


Fig. 2 Optical images of the water droplets (6–9 mg) placed on the as-prepared bulk (a–c) or cut (d) material surface. (e) Shape of water droplet on the bulk material surface with a contact angle of  $159 \pm 1^\circ$  and sliding angle of  $1 \pm 0.5^\circ$ . (f) Mirror-like phenomenon can be observed on the bulk material submerged in water. (g–j) Contact, deformation and departure processes of a water droplet suspending on a syringe with respect to the bulk material surface. The arrows represent the moving direction of the obtained bulk material.

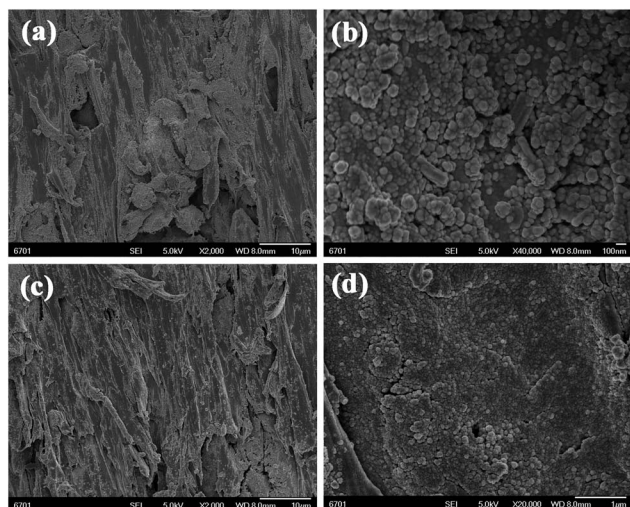


Fig. 3 FESEM images of the interior bulk material (a and b), and the bulk material surface after abrasion with sandpaper (c and d).

roughness. The bulk materials preserve the durable superhydrophobic behavior upon wear damage until they are worn out. It is found that the obtained material surface shows oil-fouling repellency, and when a drop of tetradecane is added to the surface, it is quickly drawn into the texture of the surface. After 1 h storage at room temperature, the superhydrophobic wetting behavior returns. Considering the superhydrophobic and superoleophilic properties, the bulk materials can successfully be applied to separate oil-and-water mixtures. Interestingly, under UV irradiation, the water contact angle decreases gradually, and the bulk material surface eventually

becomes hydrophilic. A reversible transition of surface wettability can be realized by alternation of UV illumination and removal of the uppermost layer upon mechanical abrasion.

The durable superhydrophobic material was prepared as follows: 1.0 g  $\text{TiO}_2$  nanorods and 1.0 g hydrophobic  $\text{SiO}_2$  nanoparticles (Fig. S1, ESI<sup>†</sup>) were dispersed in a mixed solution composed of 1,1,2,2-tetrachloroethane (40 ml) and toluene (40 ml), followed by the addition of 0.4 g vinyl-terminated poly(dimethylsiloxane) (PDMS) and stirred magnetically for about 10 min. Then, PP (4.0 g) was added into the mixed solvent and stirred for about 5 h at  $135 \pm 5^\circ\text{C}$  until PP dissolved completely. The solution was cooled and dried at ambient temperature to get the  $\text{SiO}_2/\text{TiO}_2/\text{PP}$  composite powder. The powder was placed into a mold and pressed under a pressure of 25 MPa at room temperature. After about three minutes, the sample was demolded. Herein, PDMS acts as a binder to improve the adhesion of the inorganic  $\text{SiO}_2$  and  $\text{TiO}_2$  to PP materials.

In contrast to most superhydrophobic surfaces, the liquid repellency in this work exhibits high tolerance towards mechanical damage. Abrasion of the bulk material or cutting deep into it does not result in the loss of superhydrophobicity. As shown in Fig. 2a–d, water droplets exhibit typical spherical shapes on the abrasive or cut bulk material with a water contact angle about  $158 \pm 1^\circ$  and a low sliding angle  $1 \pm 0.5^\circ$  (Fig. 2e). Upon immersion in water, the bulk material surface acts like a silver mirror when viewed at a glancing angle (Fig. 2f), due to the total reflectance of light at the air layer trapped on the surface. This trapped air can effectively prevent wetting on the material surface under water.<sup>23</sup> We analyzed the long-term durability of superhydrophobic properties under continuous contact with water (Fig. S2a, ESI<sup>†</sup>). It was found that the bulk

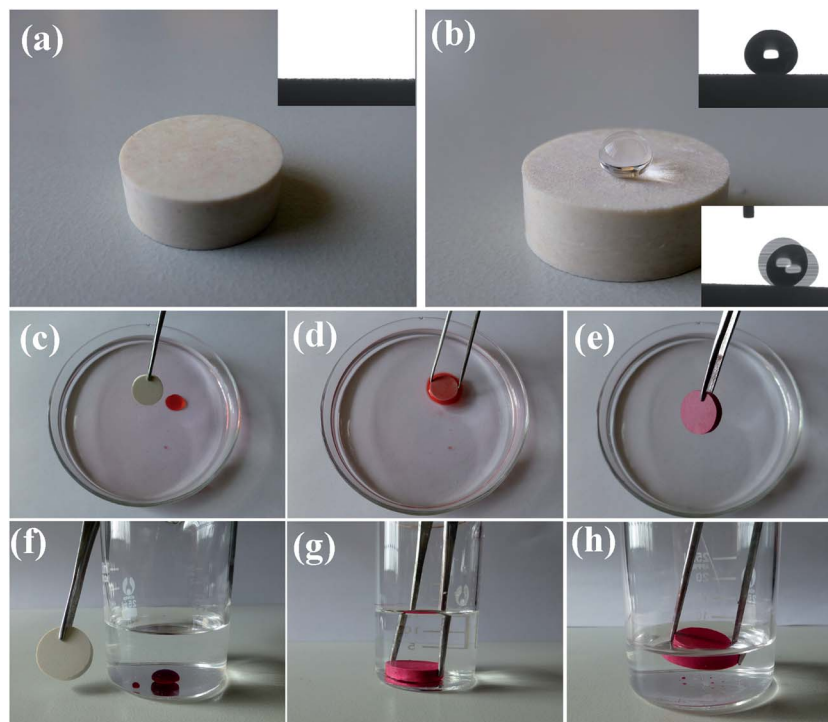


Fig. 4 (a) The spreading of tetradecane (20 mg) on the superhydrophobic material surface with oil CA value  $0^\circ$ . (b) One hour later, the coating recovered its superhydrophobicity with water CA value  $158 \pm 1^\circ$  and SA  $< 5^\circ$ . (c–h) Photographs showing the removal processes of tetradecane and chloroform from water using the as-prepared bulk material.

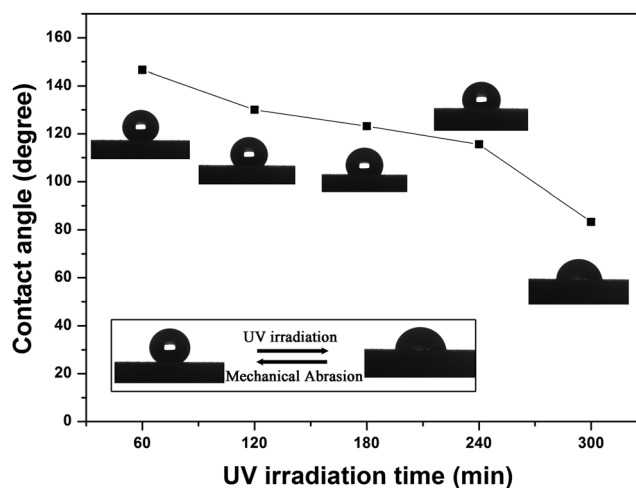


Fig. 5 Variation of water contact angle of bulk material as a function of UV irradiation time (inset is the reversible transition between superhydrophobic and hydrophilic states).

material surface still sustained the superhydrophobicity with a CA value of  $154 \pm 1^\circ$  even after being immersed in water for 3 h. When further increasing the immersion time to 5 h, the CA value decreased to  $145 \pm 2^\circ$ . It is clear that increasing the immersion time of a superhydrophobic surface in water facilitates the deterioration of contact angle values. The growth of adsorption/wetting films and hydrolysis on the material surface may be responsible for deterioration of contact angle values,<sup>23,24</sup>

and the detailed mechanisms will be discussed in ESI.† When studying the durability of the superhydrophobic bulk material, continuous contact with corrosive solution needs to be considered. Compared with pure water, corrosive solution facilitates the degradation of superhydrophobicity more easily. However, the obtained material can still sustain its water CA values  $>150^\circ$  in strong acidic solution for about 1 h, indicating good corrosion resistance (Fig. S2b, ESI†). It is interesting to note that a water droplet ( $6 \mu\text{l}$ ) suspended on a syringe can hardly be pulled down to the surface even when the droplet is squeezed (Fig. 2g–j), and movie S1 (ESI†) shows the ultra-low adhesion of the surface with water. If the water droplet happens to drop from a very short distance, it rolls off easily (SA  $< 1^\circ$ ). These observations suggest that the sliding angle is extremely low and there is very low resistance during the rolling process.

Considering the mechanical durability of the bulk material, we investigated the inner microstructure and the surface microstructure after abrasion. As shown in Fig. 3a and b, the interior of the bulk nanocomposite material contains micrometer scale roughness features that have an additional nanoscale roughness. It is believed that the nanostructure  $\text{SiO}_2$  and  $\text{TiO}_2$  aggregations affect the surface roughness, and on the other hand, hydrophobic  $\text{SiO}_2$  nanoparticles change the surface energy. Both of these factors are responsible for inducing the superhydrophobic behavior. Compared with the interior of the bulk material, the surface microstructure after mechanical abrasion has no obvious difference (Fig. 3c and d). Both the micro- and nanoscale roughness features are similar to the



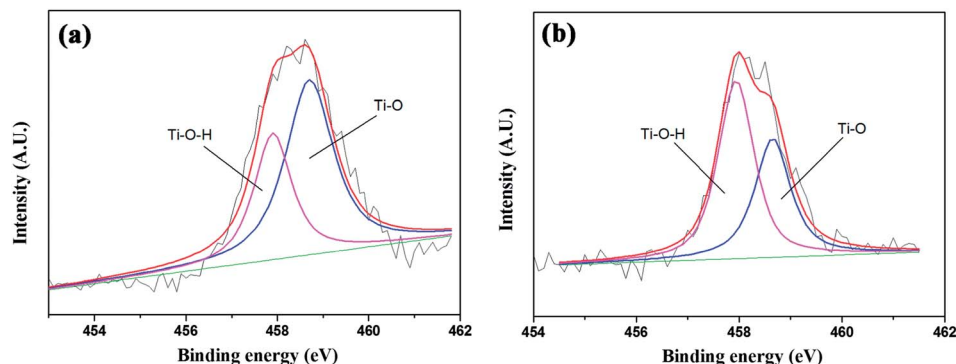


Fig. 6 Ti  $2p_{3/2}$  XPS spectra of nanocomposite bulk material surface before (a) and after (b) UV irradiation.

interior. The obtained material is tolerant to damage like a fresh surface with micro- and nanoscale topography exposed upon mechanical damage. A video of water droplets rolling off the surface after abrasion with sandpaper (800 mesh) is available in the ESI (movie S2,†), from which one can see that the abrasion process can be carried out repeatedly, each time removing a few layers of material and generating a new superhydrophobic surface which is similar to the previous one. Hence, the superhydrophobic bulk materials demonstrate mechanical abrasion resistance until they are worn out. Herein, the conventional ball-on-flat tribometer experiment was also conducted to investigate the wear behavior of the superhydrophobic bulk material (Fig. S3, ESI†).

Most superhydrophobic surfaces work well merely for hydrophilic contaminants rather than oily contaminants, since oily contaminants usually lead to the loss of superhydrophobicity. In this study, we investigated the resistance of the as-prepared bulk material to oily contaminants by using tetradecane as a control. As shown in Fig. 4, a drop of tetradecane (20 mg) spreads quickly over the surface with a contact angle of about  $0^\circ$  (Fig. 4a). That is, the bulk nanocomposite material, which demonstrates superhydrophobic behavior, also shows superoleophilicity. The water CA value decreases from superhydrophobic to hydrophobic state for the oil-fouled surface (Fig. S4, ESI†). Surprisingly, the surface regains its superhydrophobic wetting behavior ( $CA = 158 \pm 1^\circ$  and  $SA < 5^\circ$ ) after storage at ambient temperature for about 1 h. These results indicate that the superhydrophobic surfaces are resistant with regard to oil fouling. It is suggested that the tetradecane can penetrate through the structured surface due to the superoleophilicity of the bulk material. In addition, the wetting difference between water and oil on the bulk surface may provide a strategy to separate a water and oil mixture, and the oil-water separation experiments demonstrate that the bulk material can be used to separate both light oils (lower density than water) and heavy oils (higher density than water). As shown in Fig. 4c–e, the obtained materials can selectively adsorb oil floating on water surface within a few seconds, leaving a transparent region on the water surface. Fig. 4f–h shows the images of the removal process of chloroform under water. When the as-prepared sample was inserted into water to

approach chloroform, the chloroform droplet could be immediately sucked up and removed.

Tuning the surface wettability is of great interest for both scientific research and practical applications. So far, materials with tunable wettability have been developed and realized on many transition-metal oxide surfaces, such as  $TiO_2$ , ZnO, *etc.* Under UV irradiation, the hydrophobic/superhydrophobic oxide surfaces turn hydrophilic/superhydrophilic.<sup>25–29</sup> As shown in Fig. 5, under UV (obtained from a 8 W Hg lamp with a wavelength of 254 nm) irradiation, the water CA of the nanocomposite material surface decreases gradually with exposure time. After 5 h, the CA reaches a low value of  $84^\circ$ , indicating the wettability changes from superhydrophobic to hydrophilic. In order to restore the original superhydrophobicity, the UV irradiated layer just needs to be removed by mechanical abrasion to expose the interior of the superhydrophobic bulk material. Note that the switchable wettability process can be continuously repeated until the bulk material has been worn out.

To thoroughly understand the superhydrophobicity to hydrophilicity transition of the bulk material under UV irradiation, the surface compositions were examined by XPS. In fact, the mechanism for superhydrophobicity to hydrophilicity transition on transition-metal oxides has been reported previously.<sup>30,31</sup> As reported, under UV irradiation, electron-hole pairs would be generated in the valence and conduction bands of  $TiO_2$ , which could react with the absorbed  $H_2O$  and  $O_2$  molecules. This would form peroxide intermediates that could further react with the  $TiO_2$  surface to form Ti–O–H bonds.<sup>32</sup> This mechanism is consistent with the observed significant increase in the O : Ti atomic ratio (Table 1, ESI†). Fig. 6 shows the Ti  $2p_{3/2}$  XPS spectra of the bulk material surface before and after UV irradiation. The Ti  $2p_{3/2}$  peaks for  $TiO_2$  can be deconvoluted into two components at 457.9 eV and 458.7 eV, corresponding to Ti–O and Ti–O–H respectively.<sup>30</sup> After UV irradiation, the ratio of Ti–O/Ti–O–H bonding decreased from 1.2 to 0.7. The Ti–O–H groups would significantly enhance the hydrophilicity of the surface. As a result, the water CA of the nanocomposite surface decreased.

In conclusion, a nanocomposite bulk material with superhydrophobic and superoleophilic properties was fabricated by a facile approach. The material retains its superhydrophobicity even after mechanical abrasion or oil fouling. Under UV

irradiation, the surface wettability can be turned to hydrophilic, and a good reversibility of wettability is achieved through cycling between UV irradiation and removing the UV irradiated layer by mechanical abrasion. No expensive fluorochemicals are required to realize the superhydrophobicity. In contrast to most superhydrophobic surfaces that have poor durability after damage by mechanical abrasion, the presented superhydrophobic surfaces still have high water repellency with low sliding angle. It is expected that the bulk material with excellent water-repellence extending throughout its whole volume will be a new concept in designing damage-tolerant superhydrophobic materials.

## Acknowledgements

This work was supported by the Joint Talent Cultivation Funds of NSFC-HN (U1304529), National Basic Research Program of China (973 program) (Grant no. 2013CB632303), National Natural Science Foundation of China (51075120), Program for Changjiang Scholars and Innovative Research Team in University (no. PCS IRT1126).

## References

- 1 Q. F. Xu, J. N. Wang and K. D. Sanderson, *J. Mater. Chem.*, 2010, **20**, 5961.
- 2 Y. C. Jung and B. Bhushan, *ACS Nano*, 2009, **3**, 4155.
- 3 T. Wang, X. G. Hu and S. J. Dong, *Chem. Commun.*, 2007, 1849.
- 4 X. Zhang, T. Geng, Y. G. Guo, Z. J. Zhang and P. Y. Zhang, *Chem. Eng. J.*, 2013, **231**, 414.
- 5 J. Li, L. Shi, Y. Chen, Y. B. Zhang, Z. G. Guo, B. L. Su and W. M. Liu, *J. Mater. Chem.*, 2012, **22**, 9774.
- 6 X. Gao, X. Yan, X. Yao, L. Xu, K. Zhang, J. Zhang, B. Yang and L. Jiang, *Adv. Mater.*, 2007, **19**, 2213.
- 7 L. Cao, A. Jones, V. Sikka and J. Wu, *Langmuir*, 2009, **25**, 12444.
- 8 M. Ruan, W. Li, B. S. Wang, B. W. Deng, F. M. Ma and Z. L. Yu, *Langmuir*, 2013, **29**, 8482.
- 9 Q. M. Pan and M. Wang, *ACS Appl. Mater. Interfaces*, 2009, **1**, 420.
- 10 Q. M. Pan, J. Liu and Q. Zhu, *ACS Appl. Mater. Interfaces*, 2010, **2**, 2026.
- 11 X. Zhang, Y. G. Guo, P. Y. Zhang, Z. Z. Zhang and Z. S. Wu, *ACS Appl. Mater. Interfaces*, 2012, **4**, 1742.
- 12 W. X. Liang and Z. G. Guo, *RSC Adv.*, 2013, **3**, 16469.
- 13 X. Y. Zhou, Z. Z. Zhang, X. H. Xu, F. Guo, X. T. Zhu, X. H. Men and B. Ge, *ACS Appl. Mater. Interfaces*, 2013, **5**, 7208.
- 14 X. T. Zhu, Z. Z. Zhang, G. N. Ren, J. Yang, K. Wang, X. H. Xu, X. H. Men and X. Y. Zhou, *J. Mater. Chem.*, 2012, **22**, 20146.
- 15 T. Verho, C. Bower, P. Andrew, S. Franssila, O. Ikkala and R. H. A. Ras, *Adv. Mater.*, 2011, **23**, 673.
- 16 P. Roach, N. J. Shirtcliffe and M. I. Newton, *Soft Matter*, 2008, **4**, 224.
- 17 S. Höhne, C. Blank, A. Mensch, M. Thieme, R. Frenzel, H. Worch, M. Müller and F. Simon, *Macromol. Chem. Phys.*, 2009, **210**, 1263.
- 18 H. Jin, X. L. Tian, O. Ikkala and R. H. A. Ras, *ACS Appl. Mater. Interfaces*, 2013, **5**, 485.
- 19 T. Verho, C. Bower, P. Andrew, S. Franssila, O. Ikkala and R. H. A. Ras, *Adv. Mater.*, 2011, **23**, 673.
- 20 X. T. Zhu, Z. Z. Zhang, X. H. Men, J. Yang, K. Wang, X. H. Xu and Q. J. Xue, *J. Mater. Chem.*, 2011, **21**, 15793.
- 21 C. H. Su, Y. Q. Xu, F. Gong, F. S. Wang and C. F. Li, *Soft Matter*, 2010, **6**, 6068.
- 22 I. A. Larmour, G. C. Saunders and S. E. J. Bell, *ACS Appl. Mater. Interfaces*, 2010, **2**, 2703.
- 23 L. Boinovich, A. M. Emelyanenko and A. S. Pashinin, *ACS Appl. Mater. Interfaces*, 2010, **2**, 1754.
- 24 J. Groll, T. Ameringer, J. P. Spartz and M. Moeller, *Langmuir*, 2005, **21**, 1991.
- 25 I. A. Larmour, S. E. J. Bell and G. C. Saunders, *Angew. Chem.*, 2007, **119**(10), 1740.
- 26 X. Zhang, M. Jin, Z. Liu, D. A. Tryk, S. Nishimoto, T. Murakami and A. Fujishima, *J. Phys. Chem. C*, 2007, **111**, 14521.
- 27 X. Zhang, H. Kono, Z. Liu, S. Nishimoto, D. A. Tryk, T. Murakami, H. Sakai, M. Abebe and A. Fujishima, *Chem. Commun.*, 2007, 4949.
- 28 X. F. Ding, S. X. Zhou, G. X. Gu and M. J. Wu, *J. Mater. Chem.*, 2011, **21**, 6161.
- 29 Y. Liu, Z. Y. Lin, W. Lin, K. S. Moon and C. P. Wong, *ACS Appl. Mater. Interfaces*, 2012, **4**, 3959.
- 30 W. X. Hou and Q. H. Wang, *Langmuir*, 2009, **25**, 6875.
- 31 Q. F. Xu, Y. Liu and F. J. Lin, *ACS Appl. Mater. Interfaces*, 2013, **5**, 8915.
- 32 A. Weninger, J. E. Davies, K. Sreenivas and N. S. R. Sodhi, *J. Vac. Sci. Technol., A*, 1991, **3**, 1329.